High Resolution Observations of the QSO BR1202-0725:
Deuterium and Ionic Abundances at Redshifts Above z=4.

E. Joseph Wampler[1], G. M. Williger[2], J. A. Baldwin[3], R. F. Carswell[4],
C. Hazard[5] and R. G. McMahon[4]

Address for correspondence:

J.Baldwin, Cerro Tololo Interamerican Observatory, Casilla 603, La Serena, Chile.

[1]European Southern Observatory, Karl-Schwarzschild-Str. 2, D-85748 Garching bei München, Germany. Present address: National Astronomical Observatory, Osawa, Mitaka, Tokyo 181, Japan.

[2]Max-Planck-Institut für Astronomie, Königstuhl 17, D-69117, Heidelberg, Germany.

[3]Cerro Tololo Interamerican Observatory, Casilla 603, La Serena, Chile, operated by the Association of Universities for Research in Astronomy Inc. (AURA) under cooperative agreement with the National Science Foundation.

[4]Institute of Astronomy, Madingley Road, Cambridge, CB3 0HA, UK.

[5]Department of Physics and Astronomy, University of Pittsburgh, 100 Allen Hall, Pittsburgh, PA, 15260, USA.

ABSTRACT. We present results from $12 \, \mathrm{km \, s^{-1}}$ resolution echelle spectroscopy of the bright $z = 4.694$ QSO BR 1202−0725 . A preliminary analysis shows that high metallicity narrow line absorption clouds are present up to the redshift of the quasar. A damped Lyα system with an HI column density of 3.1×10^{20} cm^{-2} at $z = 4.383$ has an [O/H] ratio that is about 0.01 solar, while another absorption system with an HI column density of 5.0×10^{16} cm^{-2} at $z = 4.672$, may have an O/H ratio that is twice solar. An upper limit, or the possible detection of deuterium in this absorption cloud gives a D/H ratio of about $1.5 \, 10^{-4}$. Because this cloud is metal rich at least some of the cloud gas has been processed after the beginning of the Universe.
Key words: quasars: absorption lines — quasars: individual: BR 1202−0725 —Cosmology: observations.

1 Introduction

Element abundances at high redshift are currently of extreme interest because it is believed that at high enough redshift the element ratios will disclose the nature of the first generation of stars and their initial enrichment of the primordial gas clouds. As very efficient spectrographs that can achieve resolutions in excess of $10 \, \mathrm{km \, s^{-1}}$are now in regular use at a number of observatories, it has become practical to undertake detailed studies of the metallicity of absorption line clouds along lines of sight to distant quasars. Previous studies (see, for example, Petitjean et al. 1994) have shown that some quasar absorption-line clouds are surprisingly metal rich, even at very high redshift. However, Matteucci and Padovani (1993) have pointed out that that in its initial starburst, a galaxy can raise the metallicity of primeval clouds to nearly the solar value. They suggest that the metal enrichment of the primordial clouds might take only 5–8 10^8 years. Thus very high redshifts might be needed in order to reach look–back times that are sufficiently large that metal rich clouds are no longer found.

Also important is the abundance of deuterium at high redshift. As it is believed that deuterium is produced during the formation of the Universe and subsequently destroyed by the cycling of the initial gas clouds through stellar processes, the D/H ratio at very high redshift might be more representative of the initial deuterium abundance than that found in interstellar clouds in the Solar neighborhood. The new spectrographs now, for the first time, permit an investigation of the D/H ratio at high redshift. See Songaila et al. (1994) and Carswell et al. (1994) for previous determinations of Deuterium abundances at $z = 3.3201$.

The brightest known quasar with a redshift above $z = 4.5$ is one found during the APM optical survey for QSOs with $z > 4$ (Irwin, McMahon and Hazard, 1991). It is BR 1202−0725, which has an emission line redshift of $z = 4.694$ and magnitude R=18.7. The coordinates of this object are given in McMahon et al. (1994). Here we report on a study of absorption line systems in this object, and examine three systems with redshifts that range from $z = 4.38$ to $z = 4.69$. These are the

highest redshift absorption line clouds for which abundance studies have been reported. A previous study of this quasar (Giallongo et al. (1994)) used somewhat lower resolution to investigate the Gunn-Peterson break at the onset of the Lyα forest.

2   Observations

BR 1202$-$0725 was observed using the ESO NTT telescope and EMMI in December 1992, January 1993 and April 1994. It was also observed with the CTIO 4-meter telescope and Cassegrain echelle spectrograph at Tololo in April, 1993. For a description of the EMMI, see D'Odorico (1990). The CTIO setup was similar to that in Williger *et al.* (1994). EMMI can give a spectral resolution of about $8\,\mathrm{km\,s^{-1}}$, while the CTIO spectrograph gives a spectral resolution of about $12\,\mathrm{km\,s^{-1}}$. Integration times for the individual observations ranged from 2 hours to 3 hours. All these spectra, which have a total integration time of about 25 hours, were first transformed to vacuum wavelengths at the Solar system barycenter and then weighted by the quality of the data and combined to form the final spectrum which is analyzed here.

A Th-A lamp was used to determine the wavelength calibration of the echelle spectrum. Once a global wavelength fit to the two dimensional spectrum was found, that fit was used as a trial starting solution to identify calibration lines in the individual orders. Only unblended, moderately strong Th-A lines were used in the fits. Typically 6-10 good lines were found for each order and the resulting RMS deviation of these lines from the third order polynomial fit was about 3-5 milliangstroms. EMMI has very good wavelength stability. Wavelength drift caused by flexure or temperature changes during a two hour exposure is expected to be less than about $2\,\mathrm{km\,s^{-1}}$. The largest single uncertainty in the wavelength calibration is the uncertainty in the distribution of starlight in the 1.5 arcsec slit. If our uncertainties combine quadraticly, the velocity integrity of the spectrum should be good to about $2\,\mathrm{km\,s^{-1}}$, and we believe that the zero point of the wavelength scale has a similar accuracy. We have relied on the accuracy of this calibration over a wide wavelength range in the analysis of the spectrum. This has provided a substantial constraint on possible models of the spectrum.

By first shifting our spectra to barycenter wavelengths, we have widened and distorted the lines in our spectrum that are due to the Earth's atmosphere. It was difficult to correct the individual spectra for the atmospheric lines because we do not have observations of suitable standard stars taken at the same time and airmass as our quasar observations. We have made a crude correction of the atmospheric b-band using data from an earlier spectrum of Q 0059$-$2735 (see Wampler et al. , 1995). Q 0059$-$2735 had been observed in a very similar fashion to BR 1202$-$0725. Because

Q 0059−2735 is brighter than BR 1202−0725, the signal to noise ratio for Q 0059−2735 is higher than that of BR 1202−0725. Furthermore, in the spectrum of Q 0059−2735 there are no strong lines in atmospheric b-band spectral region. Therefore, the spectrum of Q 0059−2735 can be used to estimate the atmospheric absorption line contribution to the spectrum of BR 1202−0725. This correction is not perfect, but it is sufficient to our purposes.

Fig. 1 gives an overview of the spectrum of BR 1202−0725 (see also the spectrum, taken with lower resolution and published by Giallongo et al. 1994). Here the data have been rebinned to a resolution of 2Å. The spectrum has been normalized to a median filtered spectrum of Hiltner 600 (Stone 1977). This procedure grossly distorted the intensities near the wide atmospheric A-band, where the filter did not bridge the band, but did not significantly affect the relative intensities at other wavelengths where the absorption lines are narrower and the filter was able to smooth across the lines. In Fig. 1 the plotted intensities are in wavelength units relative to H 600.

The redshift of BR1202−0725 has been determined by Storrie-Lombardi et al. (1995, ApJ submitted) to be 4.694±0.010 based on the blue edge of the Lyα emission line. This is consistent with the peak of the Lyα emission line from our high resolution spectrum. O I λ1304, Si IV λ1400 and C IV λ1549 are the other detected emission lines (see Fig. 1). As BR1202−0725 is too heavily absorbed to use the relatively weak metal emission lines to get an accurate redshift, Storrie-Lombardi et al. used absorption features to determine the QSO redshift. This yields redshifts of 4.676 and 4.681 for OI(1304) and CIV(1549) respectively. BR1202−0725 has been detected at mm and sub-mm wavelengths (McMahon et al., 1994, Isaak et al., 1994). This emission indicates that there may be large quantities of dust within the host galaxy of BR1202−0725. We note that in quasar spectra the high ionization metal lines are often blueshifted with respect to Lyα (Gaskell 1982; Tytler and Fan 1992).

In this paper we investigate 3 metal absorption line systems in the spectrum of BR 1202−0725. These are the damped Lyα system at $z = 4.383$, and two systems near the emission-line redshift of BR 1202−0725. These latter two have redshifts of $z = 4.672$, and $z = 4.687$, respectively. There are a number of other metal-line absorption systems in the spectrum of BR 1202−0725which we have not studied in detail. The more prominent of these are listed in Table 1. In this paper we concentrate on the three systems with redshifts of $z =$4.383, 4.672, and 4.687.

3   Abundance Determinations

Column densities of the observed lines were found by modeling the spectrum using a MIDAS procedure built around a MIDAS application program called CLOUD which was written by M.

Pierre and is a derivative of the program ATLAS (Pettini *et al.* 1983). A description of the procedure used to model the lines is given by Wampler et al. (1995). The oscillator strengths used were taken from the compilation by Morton (1991). This procedure does not fit the spectrum, but many lines and components can be incorporated into the model and the resulting curve can be compared with the observed spectrum. For instance, in modeling the Lyman series in BR 1202−0725, we have used a 50-level H atom to simultaneously model the lower Lyman lines and the transition to the continuum level. Only a few of the higher Lyman lines are unblended and clearly seen in the data, but the ones that are present, together with the limits on the optical depth of the Lyman continuum and the profiles of Lyα and Lyβ are enough to constrain both the hydrogen b-values and the hydrogen column density.

It is necessary to determine the local continuum level in order to successfully model the absorption line profiles. To the red of the Lyα forest, the continuum was easily determined by running the spectrum through a 20Å wide median filter. But in the Lyα forest region, Fig. 1 shows that the local continuum is increasingly depressed as one moves to the violet. This effect is probably caused by the blending of hundreds of Lyα forest lines. In the Lyα forest region we estimated the local continuum level by assuming that the highest locations in a 100Å wide sliding band were near the continuum level. Points, selected this way, were tied together with a spline fit and the resulting smooth curve was taken to be the local continuum. The echelle spectrum of BR 1202−0725 was then divided by this continuum and the resulting normalized spectrum was used to compare with the model absorption spectrum. This procedure compensates for the continuum depression caused by overlap of many weak Lyα forest lines, but, because at a particular wavelength the local continuum may be higher than our depressed continuum, the strengths of unsaturated lines may be underestimated.

For wavelengths that are to the violet of the BR 1202−0725 Lyα emission peak, the density of Lyα absorption lines is so great that most observed absorption features are blends of more than one line. This makes modeling those metal resonance lines that lie in the Lyα forest difficult or impossible. Also, the redshift of BR 1202−0725 shifts the metal lines that lie to the red of Lyα into a wavelength region where there are many absorption lines belonging to the Earth's atmosphere. This limits our ability to determine the metallicity and ionization conditions for many of the metal-line systems found in the spectrum of BR 1202−0725. In this paper we report on three high redshift metal-line systems for which it is possible to find enough metal lines that are sufficiently free of blends with other lines to permit useful constraints to be placed on the absorption clouds. In Table 2 we list the transitions and approximate wavelengths of those transitions in the three systems that we modeled. Other lines, which can only be used to place upper bounds on the ionic column

densities, are not listed in Table 2. In Table 3 we give the hydrogen and ionic column densities, cloud velocities and Doppler line widths (b-values) for these three metal line systems. For several species our upper limits to the ionic column densities are low enough to set useful constraints to possible ionization models. We have also listed these ions in Table 3.

The following subsections contain brief descriptions of these three high redshift absorption line systems. In reading the following discussion, note that our models use fairly high b-values for several of the metal line components. Sometimes these components are clearly not saturated, yet they seem very broad. Probably these are blends of several sub-components that higher S/N and/or higher spectral resolution could resolve. However, as Jenkins (1986) has pointed out, ensembles of moderately saturated lines can be analyzed as if there were only a single component. Such an analysis gives reasonably correct results so long as the characteristics of the component clouds are not markedly irregular. With our present set of data we feel that it is best to limit the number of component clouds (and the degrees of freedom) in our model while recognizing that the actual situation may be more complex than our simplified absorption models.

3.1 System A, $z = 4.383$

The highest column density H I system in BR 1202−0725 is a low ionization system that contains several components clustered around a redshift of $z = 4.383$. We are designating it "System A". Lines of H I, O I, Si II and C II are strong, while Si IV and C IV are weak or absent at our detection limit (column densities of about $5\,10^{12}$ cm^{-2} for typical oscillator strengths). Fig. 2 shows our model fits to hydrogen Lyα and several of the metal lines in System A. Si III and N V are in the extremely rich Lyα forest region of BR 1202−0725. Given that fact that Si IV and C IV are so weak, we are doubtful that we have detected N V. Rather, it is likely that the feature at the expected location of N V is an unrelated line in the Lyα forest. Similarly, Si III may be blended with Lyα forest lines and may not be as strong as we suggest, although the presence of Si III would not be as surprising as that of N V. We have not with certainty detected *any* high ionization lines in System A.

The velocity components listed in Table 3 are those used to model the line profiles, but the true velocity structure is somewhat uncertain. We have used model fits with as few as four absorption components, and find that, unless there are some unresolved narrow saturated structures, the abundance estimates do not depend strongly on the number of assumed clouds.

The Si II column densities are based on the measurement of two lines: Si II $\lambda1304$ and Si II $\lambda1527$. These two lines limit our freedom in choosing individual cloud b-values and velocities. Given these

6

constraints, we can attempt to model the saturated O I and C II lines. The column densities listed in Table 3 are the *minimum* required to model the profiles. Saturation could possibly increase the column densities by a factor of 5 if the relative line strengths in O I and C II differed from those of Si II.

Only the total column density of H I in System A is known, not the column density of the individual clouds. The column density of H I in System A was determined by requiring that the damping wings of H I Lyα not lie below the intensity of the "continuum" region between strong lines in the Lyα forest. In this region of the spectrum our S/N ratio is about 20:1. The apparent "noise" seen in Fig. 1 is actually due mostly to many weak absorption lines. Comparing the total column density of O I with that of H I, we have estimated the abundance ratio of O/H to be about $8.3 \, 10^{-6}$, or about 0.01 solar. However, if the O I line is more saturated than we have thought, or if undetected lines in the Lyα forest have resulted in our overestimating the strength of the damping wings of the System A Lyα, then the metal abundance could be higher than our estimate.

The CII/OI and SiII/OI ratios are close to the solar abundance ratios for these elements. This suggests a photoionization model which has carbon and silicon totally dominated by the singly ionized components, so a very low ionization parameter gives the best overall fit. We used the photoionization code CLOUDY (Ferland 1995) to investigate this possibility. For a background flux of 6×10^{-21} erg cm^{-2} Hz^{-1} s^{-1} sr^{-1} the hydrogen density is 300 cm^{-3} or more if we treat the complex as a uniform density system. However, the absence of CII fine structure absorption suggests this is an overestimate by at least two orders of magnitude, and the presence of SiIV in two components is not consistent with this model. If we take the view that the SiII measurement is the most reliable (it is based on two lines), and assume a hydrogen density of 0.3 cm^{-3}, then using the background-photoionized model we find SiII/HI $\sim 1.6 \times$Si/H. SiIV is present at about 1/10 the SiII column density, as for the $z = 4.38290$ and 4.38382 components. If the OI column density is correct, then O/Si would be $\sim 1.6 \times$ solar.

We do not expect the models to be accurate to much better than a factor of two in differential abundances, and the column densities themselves are not very precise, so we do not regard such discrepancies as at all serious. In any case a small amount of dust depletion of silicon (and carbon) by an amount of order the ionization correction would readily explain the relative column densities seen for a heavy element abundance ~ 0.01 solar.

Since Al is more strongly depleted than Si in the galactic interstellar medium, a detection here with Al/Si similar to the solar value would argue against significant dust depletion of either species. Unfortunately Al II λ1670 falls in a region which is badly affected by night sky, but it is possible to determine upper limits to the Al II column density of $\sim 3.0 \, 10^{12}$ for the components at $z = 4.38382$,

4.38444 and 4.38509. Since these are upper limits, we have no handle on the dust depletion in this system. The centers of the C II λ1334 and O I λ1302 lines are saturated, so their column densities are uncertain and could be higher than the values quoted in the table. With dust depletion of Al and Si, the overall heavy element abundances could be as high as 1/25 solar.

3.2   System B, $z = 4.672$

System B appears to be dominated by absorption from a single ionized cloud at a redshift of $z = 4.67231$. In contrast to System A, the ionization conditions of System B favor high ionization clouds. Si IV is relatively strong compared to H I. C III, Si III and C IV also seem to be present, but C III and Si III lie in the Lyα forest of BR 1202$-$0725 and are blended with lines from other redshift systems. C IV is in a spectral region that has many strong atmospheric absorption lines. It is therefore difficult to measure the strengths of these lines precisely, but there are strong features at the position of the strongest component of the CIV doublet and at the wavelengths of the C III and Si III lines. Identification of the absorption features with these metal lines gives reasonable column densities.

The column density of H I in System B is quite low. This is often the case in highly ionized clouds, but there is a feature at the expected position of redshifted O I. There is no strong atmospheric line at this position, nor have we found an alternate identification for the line. If our identification of this feature with oxygen is correct, then the O/H ratio for System B is $\approx 1/500$, or twice solar. However, at the present time this identification must remain in doubt, since we have not found any evidence that C II is present. In a high ionization system the column density of C II often exceeds that of O I, because C II can exist in a H II region, while O I cannot. The upper limit to the column density of C II in System B is 10^{13} cm^{-2}, 0.1 that of O I. In contrast, we note that the C II/O I ratio in System A, a low ionization system, is 0.3, only slightly higher than the solar ratio. This might be expected in a low ionization system where the extent of the H II zone is small compared to the extent of the H I zone. Such an explanation is not likely in the case of System B, as it is a high ionization system. Nevertheless, if our O I identification is correct, it would appear that not only does System B have nearly solar oxygen abundances, but also the C/O abundance ratio is low compared to the Sun. We note that oxygen is an α-chain element that builds up in abundance very rapidly in the early universe, while carbon is an element that is co-produced with iron and builds up more slowly (Timmes et al., 1995). Thus, an overabundance of oxygen in a high redshift system might signal the extreme youth of the metal-line cloud. Petitjean et al. (1994) have commented that oxygen seems to be overabundant relative to carbon in the $z = 2.034$ system of

8

PKS 0424-131. They also find that absorption systems with high metal content are usually found to have redshifts close to that of the background quasar. They argue that such systems are physically associated with the quasar. If our identification of O I in System B is correct, this may be another example of a high metallicity system with anomalous abundances having a redshift close to that of the background quasar. However, if the observed absorption feature is not due to O I, the metal abundance of System B might be quite low.

3.3   System C, $z = 4.687$

System C, a cloud complex near redshift $z = 4.687$, is, like system B, a high ionization system with strong C IV compared to the low ionization lines. C III may also be present in this system as there is a pair of lines at the correct wavelength to give a reasonable identification with C III. Fig. 4 shows that the $^5D - ^7P$ Fe III $\lambda 1214.56$ transition may be present with measurable strength. However, this line is blended with a strong line in the atmospheric b-band. In spite of our attempt to correct the spectrum of BR 1202−0725 for absorption by the b-band, this blend causes an uncertainty in the column density of Fe III. Also, the probability of finding a hydrogen line at the expected position of Fe III is substantial, though the observed feature is somewhat too narrow to be identified as a hydrogen line. As we have found no evidence for O I in the System C clouds, and as we have no trustworthy ionization model, we cannot determine the metal abundance in this system. Our absorption model for System C uses two components: a strong, blue component with a fairly low b-value, and a red component that is weaker and wider than the blue component. More components could have been used, but our data in the C IV region, where the components are best seen, are too noisy to justify the increased complexity.

3.4   The D/H ratio

Because the high ionization clouds in System B are dominated by a single absorption component, it is well situated for investigating the D/H ratio at high redshift. Fig. 4 shows the Lyα and Lyβ lines and the higher order Lyman lines for both System B and System C.

The hydrogen column densities of Systems B and C are constrained by the observational data in three ways: (1) by the width and shape of Lyα and Lyβ; (2) by the point at which the higher Lyman lines stop being saturated; and (3) by the residual continuum level below the Lyman break.

The widths and shapes of the first two Lyman lines are relatively unaffected by blends with other lines, as can be seen in Figure 4. The point at which the Lyman lines stop being saturated can be judged from Figure 5, which shows an expanded view of the spectral region where the transition

from the Lyman lines to the Lyman continuum in the two systems occurs. While the high order Lyman lines fall in a spectral region that is highly confused by blends with other features, there are, nevertheless, numerous sections of the BR 1202−0725 spectrum where the System B and C Lyman lines leave a clear imprint. The Lyman-15 transition is designated by the numeral 15 directly under the appropriate system. Since in our model, System C has two components, we have placed the letter designating lines in this system between the two components. Even though the location of the appropriate continuum is uncertain, the fact that there is little residual intensity until we reach absorption lines that are high in the Lyman series means that the Lyman lines are saturated until ∼Ly15. Because the b-value required to fit the lower Lyman lines decreases as the assumed column density increases, the model lines in the higher Lyman series strengthen and narrow as the column density increases.

Figs. 1 and 5 demonstrate that there is significant residual continuum in the spectrum of BR 1202−0725 below the Lyman limits of these two absorption systems. In fact, there is substantial residual continuum shortward of the System B limit at 5180Å to about 5000Å where the flux is cut off by a different system. However, because the exact location of the local continuum is uncertain, the depression of this continuum by the Lyman continuum absorptions of systems B and C is probably a less secure method of determining the hydrogen column density than noting that we see saturated Lyman lines to very high n-values. The presence of these saturated higher Lyman lines sets a lower limit to the hydrogen column density of the clouds, while the residual continuum in the spectrum of BR 1202−0725 sets an upper limit to this column density. For the hydrogen column densities found for systems B and C, the depth of the continuum absorption should be about 60% of the continuum level in the Lyman series. That this amount of absorption is about correct can be best seen in the overview given in Fig. 1 (the spectrum of BR 1202−0725 in this region is not as noisy as it may appear; there are a very large number of blended absorption lines in this spectral region and they contribute substantially to the irregularity in the spectral flux).

Constrained by the observed Lyman continuum flux, the strengths of the higher Lyman lines, and the profiles of Ly-α and Ly-β, and taking into account the first 50 Lyman lines, we iteratively modeled the hydrogen spectra of Components B and C. Because the Lyman continuum of System C overlaps the higher order Lyman lines and continuum of System B, we first determined the bounds on the system C hydrogen column density and then with the System C continuum in place, we adjusted the continuum level for System B. We were thus able to model System B in the presence of absorption by System C. Once the hydrogen column densities had been established for the two systems, we adjusted the component b-values (one for System B and two for System C) in order to provide acceptable models for the lower Lyman lines. The b-values required to model the observed

10

profile are very sensitive to the assumed column densities, so it is not possible to estimate the column density using only the lower, saturated, Lyman lines. In BR 1202−0725 we are fortunate that the spectrum gives us enough constraints to determine the required parameters. We believe that the model shown in this figure and listed in Table 3 is conservative. Models with twice the hydrogen column density would not fit as well, but might be acceptable. Decreasing the H I column density by factor of two would require a large number of chance coincidences of unrelated absorption lines with the positions of the Lyman series lines. We feel that such a large number of coincidences would be very unlikely.

The observed Lyα lines of both System B and System C show small dips at the expected location of D I. These positions are designated in Fig. 4. Because there is a possibility that weak, satellite H I features cause the depressions, we can only determine upper limits for the D/H ratios in these clouds. The position of $D_{Ly\alpha}$ in System B is free of strong atmospheric b-band absorption lines, but the $D_{Ly\alpha}$ line in System C is blended with an atmospheric b-band line. Of course, in System C the only D I line that we could see is the one due to the blue (and strongest) component of the two lines in our model. The D I line belonging to the red component is lost in the absorption due to the blue H I component. It is unfortunate that not only is the $D_{Ly\alpha}$ in System C blended, but the $D_{Ly\beta}$ line in System C is also confused with other absorption features. We find that D/H $\lesssim 1.5\,10^{-4}$ for System B and D/H $\lesssim 10^{-3}$ for System C, for the reasons just given, the latter value is extremely uncertain. In calculating the D/H ratios, we have taken our best estimate for the hydrogen column densities. If we had taken the upper limit, we could have decreased the D/H ratios by a factor of about two. Without better data it is not possible to make a stronger statement. However, we note that the D/H ratio derived for System B is similar to that ($\lesssim 2\,10^{-4}$) found by Songaila et al. (1994) and Carswell et al. (1994) for the quasar Q 0014+813.

The upper limit that we find for the D/H ratio in System B ($\lesssim 10^{-4}$) is very close to the primordial ratio predicted by the calculations for the first creation of the light elements during the formation of the Universe. The initial D/H ratio depends on the baryon-to-photon ratio η and decreases as η increases. As the primordial gas is processed by stars, the D/H ratio can only decrease with time as it is believed that there are no efficient processes to increase the deuterium abundance after the big bang. For a discussion of the decrease of D/H with time see (Vangioni-Flam et al. , 1994, and Steigman and Tosi, 1992). The value of η can be determined from the primordial ^{4}He mass fraction (Y_p). For $Y_p \approx 0.23 \pm 0.01$ (Olive et al. , 1991; Pagel et al. , 1992) $2.8\,10^{-10} \leq \eta \leq 4.2\,10^{-10}$ (Vangioni-Flam et al. , 1994). Calculations show that for $\eta = 4\,10^{-10}$, $(D/H)_p = 5\,10^{-5}$. this increases to $(D/H)_p = 8\,10^{-5}$ for $\eta = 3\,10^{-10}$.

Our systems B and C are at very large redshifts, they are thus "pre-solar". However, we do

not know the fractional gas content of each cloud that is primordial. For instance, they might even be supernova remnants, in which case the D/H ratio should be very small. However, as both clouds show a weak feature near the expected position of D I we may have actually detected D I. Clearly these two systems merit further study, to improve both the H I and D I column densities. An increase in the S/N ratio at Lyβ might lead to a detection of D Lyβ in System B. This would improve the accuracy of the column density measurement of D I and might provide an independent estimate of cloud b-values for the light atoms.

4 Conclusions

We find that even at redshifts in excess of 4, it is possible to find intervening quasar absorption systems with strong metal lines. We identify three such systems, A ($z = 4.383$), B ($z = 4.672$) and C ($z = 4.687$). Of the three systems studied here, System A has the most reliable abundance determination. We estimate that for it, the O/H abundance is at least ~ 0.01 times solar. System B ($z = 4.672$) may be even more metal rich if our identification of an isolated weak line with oxygen is correct. The O/H abundance in System B may be ~ 2 times solar (although this would seem to require a very low C/O abundance ratio).

High metallicity at large redshift requires a short delay time (τ_{delay}) between the start of the universe and the beginning of galaxy formation. Timmes et al. (1995) have used published quasar abundances to argue that the data are compatible with τ_{delay} of the order of 3 Gyr for universes with $\Lambda = 0$ and Ω between 0.2 and 1. From our data τ_{delay} must be less than 1 Gyr if their assumptions concerning the Universe are correct. In fact, the metallicity we find in the three absorption systems that we have analyzed in BR 1202−0725 is not qualitatively different from the systems found at much lower redshift.

Deuterium may have been found in System B. If so, the abundance is similar to that found earlier in the $z = 3.32$ system of Q 0014+813 by Songaila et al. (1994) and Carswell et al. (1994).

5 Acknowledgments

this paper.

REFERENCES

Carswell R.F., Rauch M., Weymann R.J., Cooke A.J., Webb J.K., 1994, MNRAS 268, L1

D'Odorico S., 1990, *The Messenger* 61, 51

Ferland G.J., 1995, *Hazy, a Brief Introduction to Cloudy*, University of Kentucky Physics Department Internal Report

Gaskell C. M., 1982, ApJ 263, 79

Giallongo E., D'Odorico S., Fontana A., et al., 1994, ApJ 425, L1

Irwin M.J., McMahon R.G., Hazard C., 1991, in: Crampton D. (ed.), ASP Conf. Ser. Vol. 21, The Space Distribution of Quasars. Astron. Soc. Pac., San Francisco, p. 117.

Jenkins E.B., 1986, ApJ 304, 739

Matteucci F., Padovani P., 1993, ApJ 419, 485

McMahon R.G., Omont A., Bergeron J., Kreysa E., Haslam C.G.T., 1994, MNRAS 267, L9

Morton D.C., 1991, ApJS 77, 119

Olive K.A., Steigman G., Walker T.P., 1991, ApJ 380, L1

Pagel B.E.J., Simonson E.A., Terlevich R.J., Edmunds, M.G., 1992, MNRAS 255, 325

Petitjean P., Rauch M., Carswell R.F., 1994, A&A 291, 29

Pettini M., Hunstead R.W., Murdoch H.S., Blades, J.C., 1983, ApJ 273, 436

Songaila A., Cowie L.L., Hogan C.J., Rugers, M., 1994, Nature 368, 599

Steigman G., Tosi M., 1992, ApJ 401, 150

Stone R.P.S., 1977, ApJ 218, 767

Storrie-Lombardi L., McMahon R.G., Irwin M.J., Hazard C., 1995, ApJ, submitted

Timmes F.X., Lauroesch J.T., Truran J.W. 1995, ApJ 451, 468

Tytler D., Fan X.-M., 1992, ApJS 79, 1

Vangioni-Flam E., Olive K.A., Prantzos N., 1994, ApJ 427, 618

Wampler E.J, Chugaǐ N.N., Petitjean, P., 1995, ApJ 443, 586

Williger G.M., Baldwin J.A., Carswell R.F., et al., 1994, ApJ 428, 574

TABLE 1 Metal-Line Systems in BR 1202−0725

$\lambda_{obs,vac}$	W_{obs}	ION	λ_{lab}	z
7152.6	2.4	Fe II	2586	1.7546
7162.6	3.3	Fe II	2600	1.7546
7702.7	5.5	Mg II	2796	1.7546
7722.8	5.4	Mg II	2803	1.7546
8428.4	1.8	Mg II	2796	2.0141
8450.1	0.6	Mg II	2803	2.0141
8068.5	2.9	Fe II	2344	2.4420
8172.2	1.6	Fe II	2374	2.4420
8201.4	3.7	Fe II	2382	2.4420
8900.4	2.4	Fe II	2586	2.4420
8948.5	4.5	Fe II	2600	2.4420
7070.8	1.1	Si IV	1393	4.0734
7116.7	0.6	Si IV	1402	4.0734
7854.9[1]	3.0	C IV	1548	4.0734
7867.7	1.8	C IV	1550	4.0734
8384[2]	1.0	C IV	1548	4.4126
8394[2]	0.5	C IV	1550	4.4126
8486[2]	3.0	C IV	1548	4.4811
8499[2]	1.8	C IV	1550	4.4811

[1]Noise spike in line.

[2]At least two velocity components, structure not determined.

15

TABLE 2. List of Modeled Line Complexes

	SYSTEM A $z = 4.383$					
$\lambda_{obs,vac}$	6544	7184	7010	7022	8219	6494
$W_\lambda^{obs}(\text{Å})$	65	3.76	3.97	1.21	2.20	3.33
Ident	Lyα	C II	O I	Si II	Si II	SiIII

	SYSTEM B $z = 4.672$				
$\lambda_{obs,vac}$	6896	5818	7386	7906	8782
$W_\lambda^{obs}(\text{Å})$	3.11	2.15	0.33	0.47	0.64
Ident	Lyα	Lyβ	O I	Si IV	C IV

	SYSTEM C $z = 4.687$				
$\lambda_{obs,vac}$	6914	5833	6908	7927	8806
$W_\lambda^{obs}(\text{Å})$	6.38	4.49	0.4:	0.83	3.44
Ident	Lyα	Lyβ	Fe III	Si IV	C IV

Table 3. Cloud Column Densities

Sys.	Z	b(H I)	H I[1]	D I	b(metals)	C II	C III	C IV
A	4.38133				10	3.3E13		≲ 1E13
A	4.38192				10	3.2E13		≲ 1E13
A	4.38250				10	5.6E13		≲ 1E13
A	4.38290		3.1E20		12	3.6E14		≲ 1E13
A	4.38382				30	3.8E14		≲ 1E13
A	4.38444				20	8.0E13		≲ 1E13
A	4.38509				12	8.0E13		≲ 1E13
B	4.67231	22	5.0E16	≲ 8.0E12	15		≲ 2.0E14	4.0E13:
C	4.68664	25	1.4E16	≲ 2.5E13	20		2.0E14:	2.0E14
C	4.68831	45	7.2E15		30		5.0E13:	1.5E14

Sys.	Z	b(metals)	N V	O I	Si II	Si III	Si IV	Fe III
A	4.38133	10		8.8E13	≲ 4.0E12	≲ 1.5E12		
A	4.38192	10		8.0E13	≲ 4.0E12	≲ 2.0E12		
A	4.38250	10		1.4E14	7.0E12	≲ 3.0E14		
A	4.38290	12	≲ 8.0E13	9.0E14	4.5E13	≲ 6.0E13	≲ 1.0E13	
A	4.38382	30	≲ 8.0E13	9.6E14	4.8E13	≲ 2.0E13	≲ 1.0E13	
A	4.38444	20		2.0E14	1.0E13	≲ 1.0E12		
A	4.38509	12		2.0E14	1.0E13	≲ 5.0E12		
B	4.67231	15		1.0E14		≲ 8.0E12	1.2E13	
C	4.68664	20				≲ 3.0E14	1.5E13	≲ 1E16
C	4.68831	30				≲ 2.0E12	5.0E12:	≲ 2E15

[1]Only the total column density of H I in System A is known, not its distribution among the individual clouds.

FIGURE CAPTIONS

Fig. 1. — Overview of the spectrum of BR 1202−0725 rebinned to 2Å per bin. The positions of several strong emission lines are marked. 9 pixels with values below -1 have been assigned the value -1, and 1 pixel with a value greater that 18 has been assigned the value 18. The flux is relative to that of Hiltner 600.

Fig. 2. — The damped Lyα line of the low ionization system A, together with several of the metal lines. Because there is severe blending with Lyman lines in other redshift systems, the N I , N V and Si III features are considered only to be upper limits to the true column densities.

Fig. 3. — Selected metal absorption lines in systems B and C.

Fig. 4. — The Lyman series of H I for systems B and C. The maximum column density of system C is set by the requirement there not be too much absorption in the interval between 5180 Å and 5200 Å. The maximum column density of system B is set by a similar requirement for the Lyman continuum region below 5180 Å. The numeral "15" indicates the location of the Lyman-15 transition.

Fig. 5. — Details of the higher Lyman lines for Systems B and C. The numeral "15" indicates the location of the Lyman-15 transition.
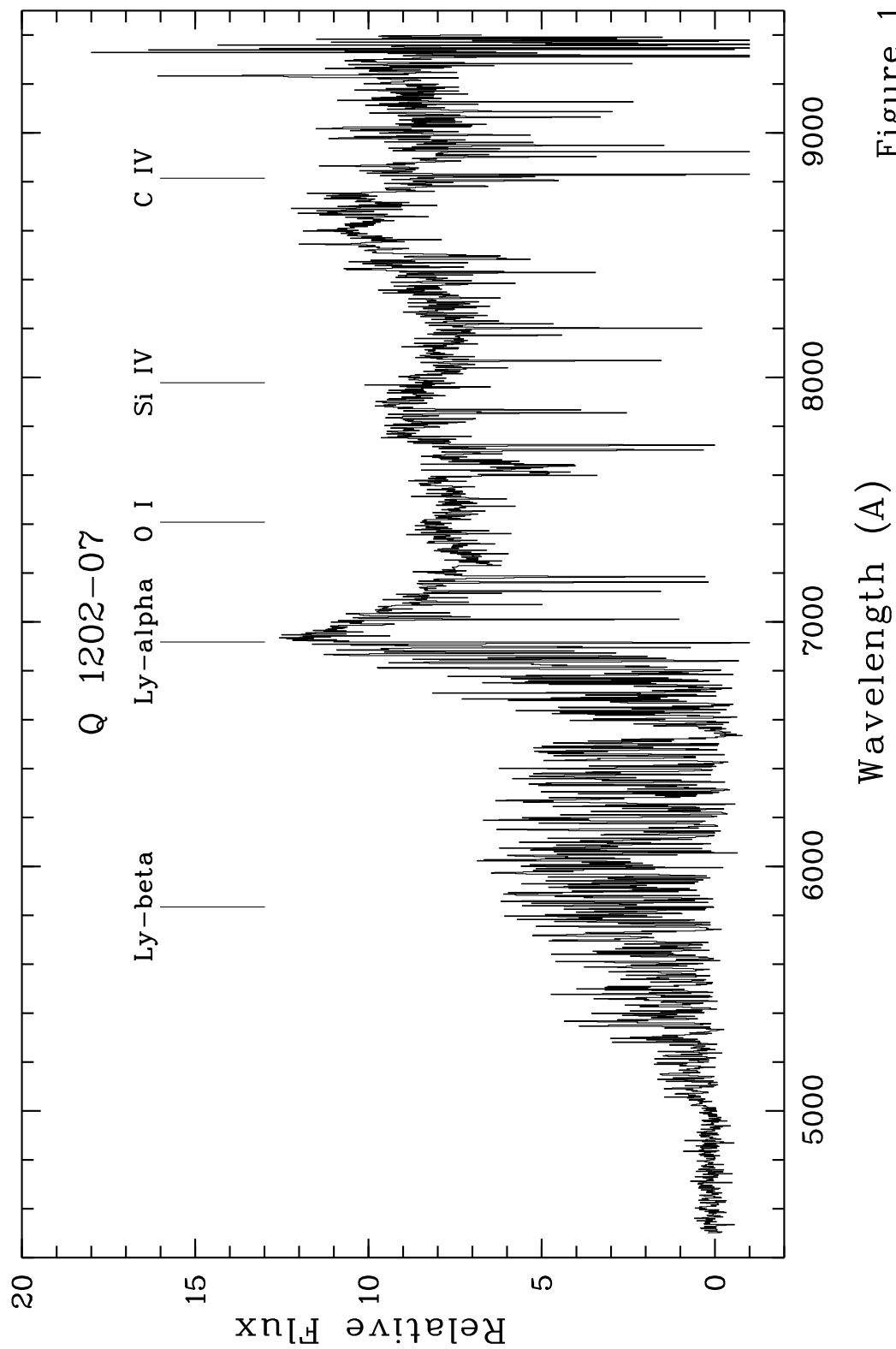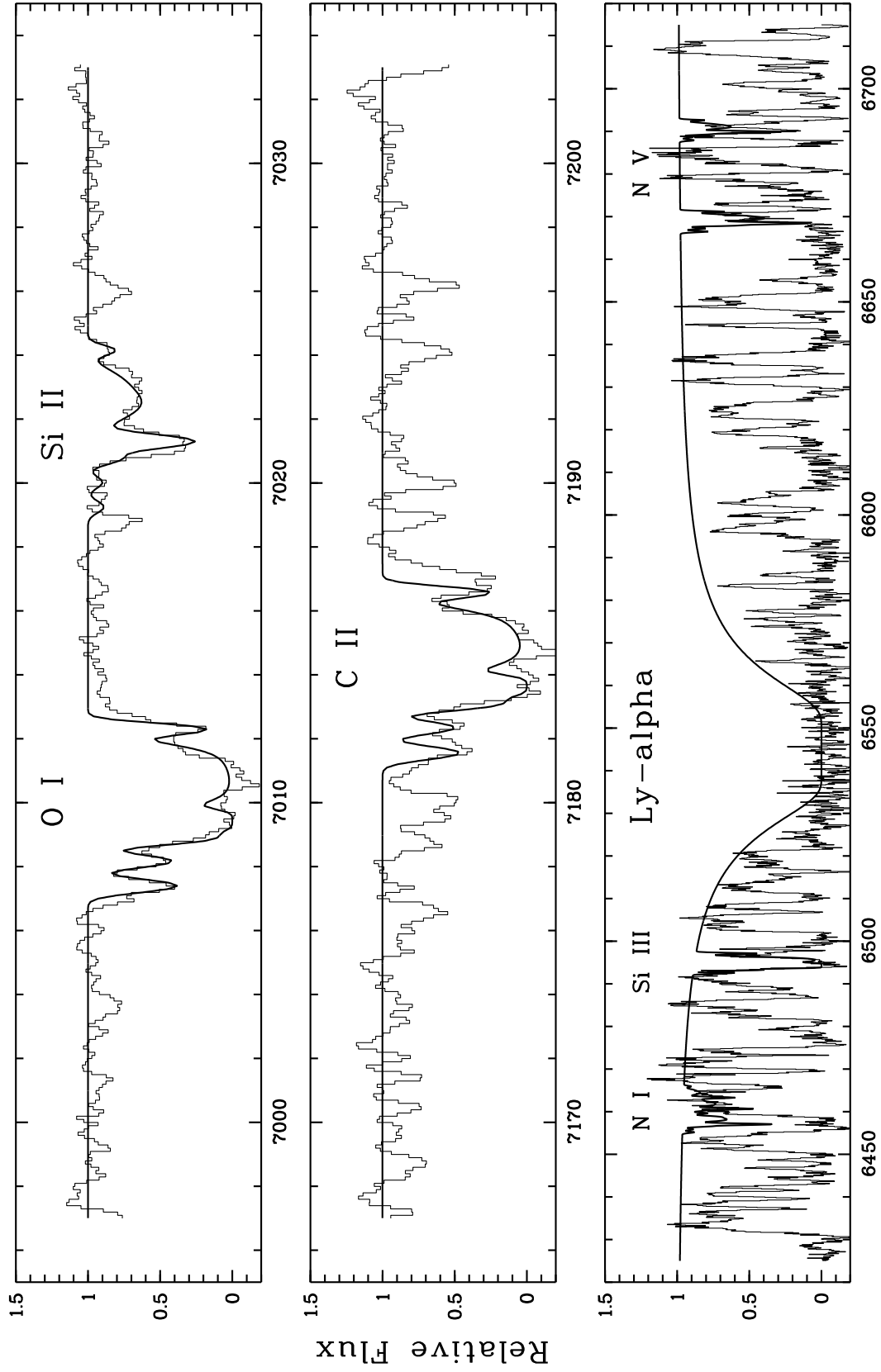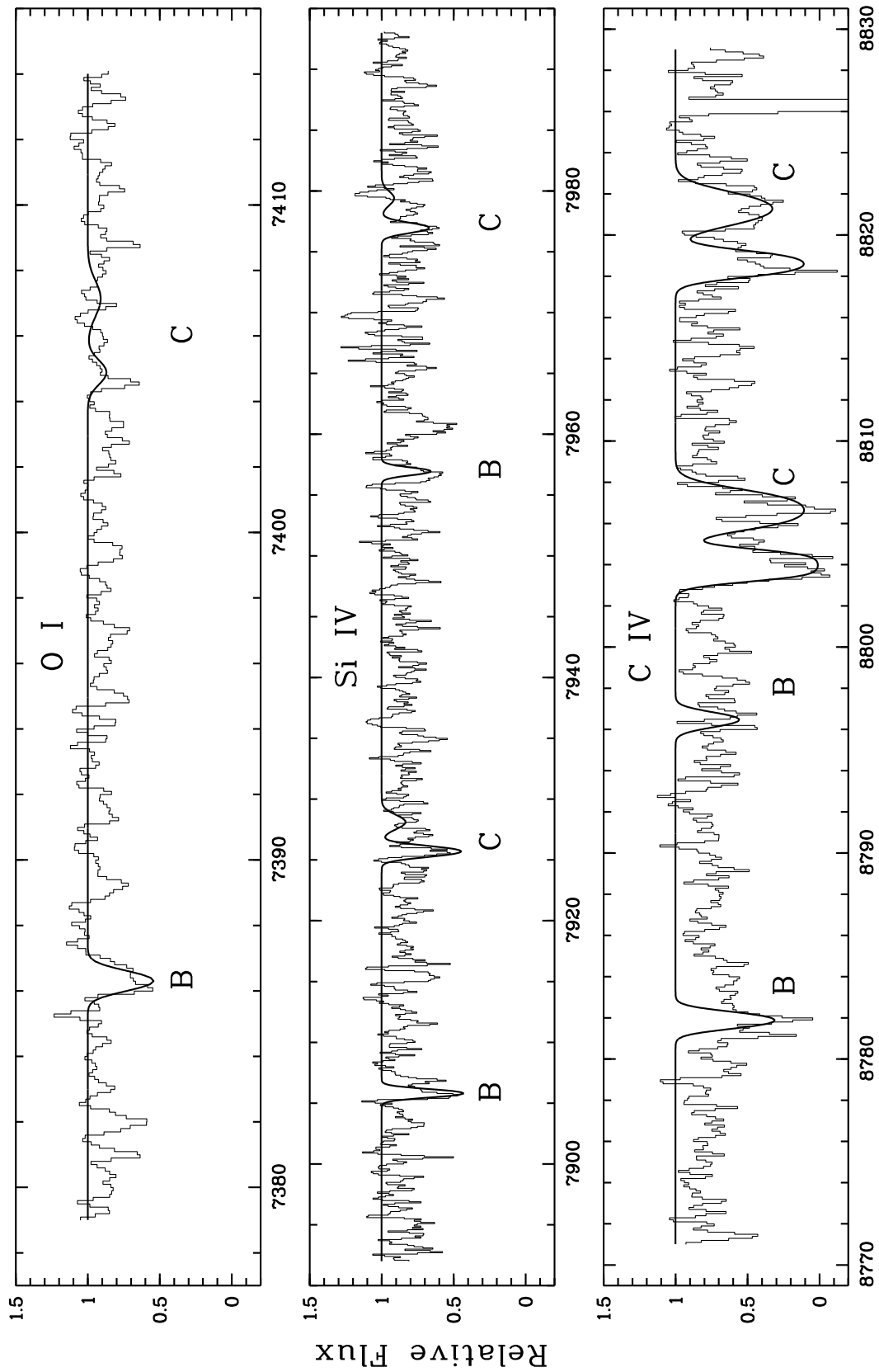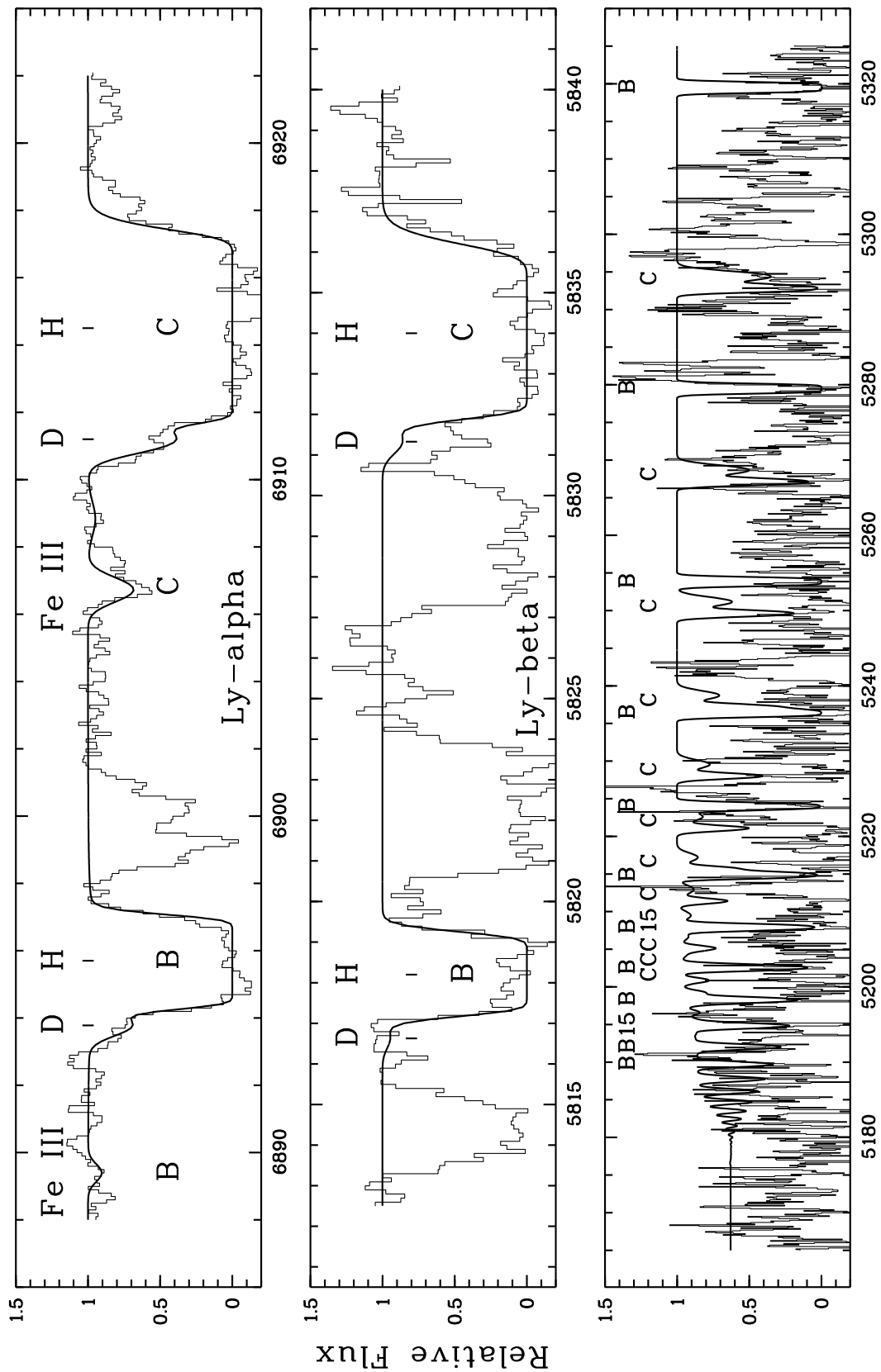
Figure 1

Figure 2

20

Figure 3

21

Figure 4

Figure 5